

Explainable Biomedical Recommendations via Reinforcement Learning Reasoning on Knowledge Graphs

Gavin Edwards¹

GAVIN.EDWARDS@ASTRAZENECA.COM

Sebastian Nilsson²

SEBASTIAN.NILSSON@ASTRAZENECA.COM

Benedek Rozemberczki¹

BENEDEK.ROZEMBERCZKI@ASTRAZENECA.COM

Eliseo Papa¹

ELISEO.PAPA@ASTRAZENECA.COM

¹Biological Insight Knowledge Graph (BIKG), Research D&A, R&D IT, AstraZeneca, Cambridge, UK

²Biological Insight Knowledge Graph (BIKG), Research D&A, R&D IT, AstraZeneca, Gothenburg, Sweden

Abstract

For Artificial Intelligence to have a greater impact in biology and medicine, it is crucial that recommendations are both accurate and transparent. In other domains, a neurosymbolic approach of multi-hop reasoning on knowledge graphs has been shown to produce transparent explanations. However, there is a lack of research applying it to complex biomedical datasets and problems. In this paper, the approach is explored for drug discovery to draw solid conclusions on its applicability. For the first time, we systematically apply it to multiple biomedical datasets and recommendation tasks with fair benchmark comparisons. The approach is found to outperform the best baselines by 21.7% on average whilst producing novel, biologically relevant explanations.

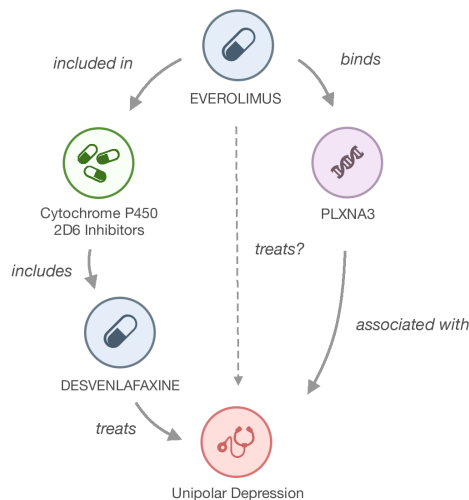


Figure 1: Transparent reasoning for why Everolimus could treat Unipolar Depression.

1. Introduction

Drug development costs are ten times what the industry spent per year in the 1980s and continuously growing. The average new drug is now expected to take ten or more years to develop and cost over \$2 billion (Austin and Hayford, 2021). To improve on this trend, there is increasing interest in enhancing human decision making with Artificial Intelligence (AI) recommendation systems.

AI recommendation systems commonly use black-box models that solely focus on optimising performance for tasks such as product recommendation and personalised content. These are high-frequency, low-risk recommendations that receive fast feedback to improve and build trust. However, the application of

recommendations in the drug discovery space suffers from significant limitations (Gogleva et al., 2021): decisions are infrequent, high-risk and can have a large impact.

AI may pave the way for innovative new therapies, but pursuing the recommendations means devoting time and resources. First, experts are needed to label and rank recommendation lists, and then laboratory scientists must undertake costly and often time-consuming experiments to provide further validation. Finally, stakeholders need to persevere when provided recommendations are not successful, which

is certain to happen, given the notoriously high failure rates of new drugs. The whole process demands robust, sustained trust from humans. Therefore, a human-centric approach is essential. We argue that, in tandem with accurate recommendations, providing transparent reasoning, as shown in Figure 1, is a key part to building the trust required.

Drug discovery recommendation tasks include, but are not limited to, drug repositioning, disease target identification and personalised medicine. Some recent successes have been obtained in the application of recommendation systems on top of networks and knowledge graphs of biological knowledge (Barabási et al., 2011). For instance, machine learning models trained on graphs have been used to find novel drug candidates for COVID-19 (Zhou et al., 2020; Gysi et al., 2021), identify efficacious drug combination therapies (Cheng et al., 2019) and discover novel drivers of drug resistance (Gogleva et al., 2021).

A Knowledge Graph (KG) is a data representation that links diverse types of data together into a single, unified model. It enables complex and nuanced relationships to be captured. Due to the increasing breadth and depth of biomedical data, biomedical KGs have become a popular way to integrate the complex and diverse data into a single unified representation.

Biomedical KGs can contain and integrate data ranging from disease networks and protein interactions to healthcare records and scientific knowledge extracted from literature. The intrinsic patterns, uncertainty and bias within biomedical data presents many unique challenges for reasoning (Bonner et al., 2021). Biomedical KGs are also structurally different from standard KGs (Figure 4). Because of this, the common assumptions and methods for graph reasoning often fail to generalise (Liu et al., 2021).

1.1. Main contributions:

This paper makes the following novel contributions:

1. Applying multi-hop neural-driven recommendation to complex biomedical KGs 10x bigger than previously used.
2. Benchmarking multiple algorithms on representative biomedical datasets and tasks with standardised evaluations.
3. Validating if biologically relevant explanations are produced with biomedical expert end users.

4. Finding that multi-hop reasoning has the potential to generate explanations and boost the performance of black-box methods.

2. Related Work

2.1. Knowledge Graphs

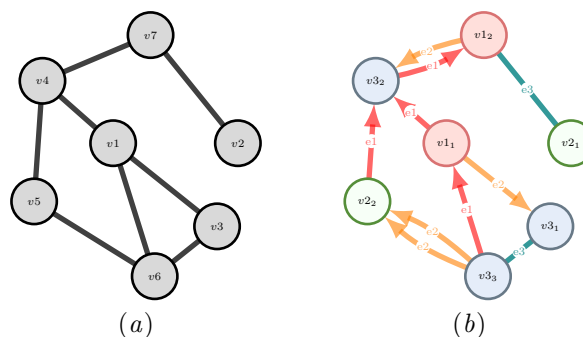


Figure 2: Basic graph (a) vs knowledge graph (b)

At the fundamental level, graphs contain information about a set of entities (also referred to as nodes or mathematically as vertex) and the set of relationships (also known as edges) between them. A Knowledge Graph (KG) is a heterogeneous, multi-relation graph that can contain directed and undirected edges. This means it has many types of entities and relations, can have multiple edges of the same type between entities, and the edges may indicate direction (Figure 2).

The core component of a graph is a triple. A single triple defines how two entities are linked. It consists of a head entity h , relation r and target entity t . A triple is therefore defined by (h, r, t) . An example of a triple would be $(London, capital\ of, United\ Kingdom)$. When multiple triples are combined, it creates a graph.

A common graph reasoning task is link prediction. It is used to discover new links within incomplete KGs. Many classical AI problems such as recommendations, reasoning and question answering can be rephrased as link prediction problems. The task is to find new links by identifying entities that correctly complete a query. For example, predicting drugs to treat COVID-19 could be defined as finding tail entities that correctly complete the triple $(COVID-19, treated\ by, ?)$.

In industry, KGs have been successfully deployed in many applications such as search engines, social graphs, fraud detection and product recom-

mentation. KGs commonly used for benchmarking within research include FB15K-237 (Toutanova et al., 2015), NELL-995 (Xiong et al., 2017) and WN18RR (Dettmers et al., 2018).

However, the lack of large and reliable benchmark graphs for research purposes is well known (Hu et al., 2020). In particular, standard, representative and fair benchmark graphs are still limited for specialist problems such as biomedical recommendation. Initiatives such as the Open Graph Benchmark (Hu et al., 2020) are good attempts at solving this, but still not representative of large biomedical KGs used in industry. OGB’s biomedical KG is relatively small and has only 5 node types (Appendix A.3). It also differs structurally when compared to the low degree graphs with NLP edges extracted from literature (Figure 4).

2.2. Biomedical Knowledge Graphs

Biomedical KGs are a specialist type of KG that focus on the biomedical domain. They include information between entities such as genes, diseases, pathways and compounds. The data is usually collected from a wide variety of data sources (Bonner et al., 2021). An example ontology can be seen in Figure 3. The biomedical data is large, noisy, incomplete and contains contradictory observations. Structurally, the graphs exhibit long-range dependencies, many high-degree hub entities, a higher density of links, long tails of weakly connected entities and higher heterogeneity than standard benchmark graphs (Figure 4).

Biomedical KGs are becoming increasingly popular within industry and as open-source initiatives. Examples include, BioKG (Walsh et al., 2020), DRKG (Ioannidis et al., 2020), Clinical KG (Santos et al., 2020), Hetionet (Himmelstein et al., 2017), OpenBioLink (Breit et al., 2020), OGBL-BIOKG (Hu et al., 2020) and PharmKG (Zheng et al., 2020b).

2.3. Existing Reasoning Approaches

Existing approaches to reasoning on KGs originate from different theoretical perspectives with varying levels of explainability. The approaches can be categorised into symbolic, neural and neurosymbolic reasoning approaches (Zhang et al., 2021).

Symbolic Symbolism assumes symbols are the fundamental unit of human intelligence. It treats cognition purely as a series of inferences upon symbolic representations (Haugeland, 1989). Symbolic reason-

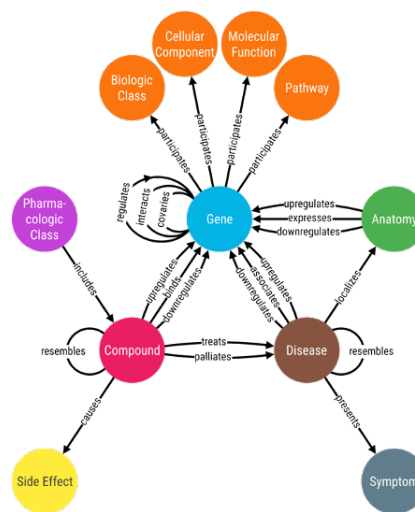


Figure 3: Ontology of Hetionet biomedical knowledge graph (Himmelstein et al., 2017). Source: <https://het.io/about/>

ing approaches deduce general logic rules to use when predicting new links.

Importantly, as they follow clear symbolic rules, the reasoning is fully transparent to the user. AnyBURL (Meilicke et al., 2019) and pLogicNet (Qu and Tang, 2019) both involve the learning of rules. Recent updates to AnyBURL added a more neuro-symbolic style. They were shown to yield impressive but not superior performance on the biomedical KG Hetionet (Liu et al., 2021).

Due to the strict matching and discrete logic operations, symbolic methods are thought to be intolerant to the ambiguity and noise of biomedical data. However, the inflexible rules can restrict the expressiveness. Additionally, it was hypothesised that large amounts of high-degree entities makes the learning and applying of logical rules more difficult (Liu et al., 2021).

Neural In contrast, connectionism is subsymbolic and imitates the neurons within brains to build models (Rosenblatt, 1958; Rumelhart et al., 1986). Instead of symbolic representations, neural reasoning approaches map entities and edges in KGs to low-dimensional vector representations known as embeddings. This approach is the focus of a large body of recent research (Wu et al., 2020).

Despite achieving state-of-the-art results on benchmark tasks, a fundamental problem with the neural

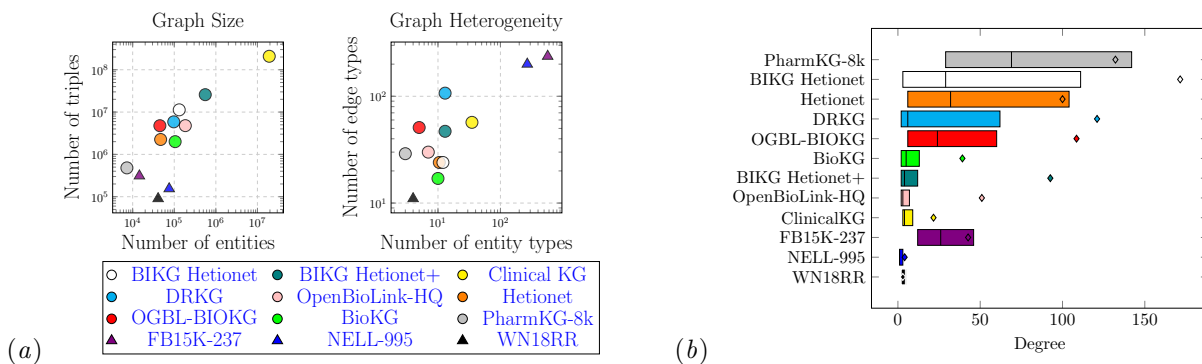


Figure 4: Comparison of biological and generic KG datasets. **(a)** *Graph size and heterogeneity*. Triangles (Δ) represent benchmark KGs, circles (\circ) note biomedical KGs. **(b)** *Skewness of degree distribution*. Box plots represent the quartiles of the degree distributions and the mean degree is denoted by the diamonds (\diamond). Biomedical KGs have a highly skewed degree distribution caused by a long-tail of poorly connected entities and a large number of highly connected hub-like entities.

approach is its non-transparent nature. Predictions are single-hop within vector space and the contributing features driving the prediction are hidden to humans.

Traditional embeddings methods are trained to minimise the reconstruction error in the immediate first-order neighbourhood while discarding higher-order proximities. There is also a homophily assumption in proximity preserving embeddings. However, most explanatory metapaths for drug repurposing were found to have length two or more (Liu et al., 2021) and biomedical graphs display heterophily.

More recently, Graph Neural Networks (GNNs) learn node embeddings by aggregating incoming messages from neighbouring nodes. In theory, these methods are capable of modeling longer-term dependencies. However, in the presence of many high-degree nodes, like in biomedical KGs, the size of neighbourhoods leads to many uninformative signals and causes over-smoothing (Kipf and Welling, 2016).

GNNs are also limited by poor expressiveness of long-tail entities with small neighbourhoods (Guo et al., 2019). This is common in biomedical KGs, demonstrated by the average degree’s 25th percentile of just 3 neighbours and positive skews in Figure 4.

Neurosymbolic The neural-symbolic approach attempts to synergise the neural and symbolic approaches. It is being increasingly referred to by the colloquial term "neurosymbolic". In graph reasoning, this leverages a symbolic graph representation to reduce the search space, cleanse uninformative sig-

nals and provide interpretability, whilst using neural approaches to increase expressiveness and adapt the reasoning to ambiguity.

These attributes are highly relevant for reasoning on biomedical KGs. Multi-hop reasoning with neural networks, a path based approach to KG reasoning, falls into the subcategory of neural-driven symbolic reasoning.

2.4. Reinforcement Learning Reasoning

Formulating KG reasoning as a neural-driven multi-hop problem naturally lends itself to Reinforcement Learning (RL). RL is known to be effective in using neural approaches for solving sequential decision-making problems. Alternative neurosymbolic approaches such as NTP (Rocktäschel and Riedel, 2017) and Neural LP (Yang et al., 2017) fail to scale to large knowledge graphs (Liu et al., 2021).

RL methods have achieved superhuman levels of performance in sequential decision making, famously for arcade games (Mnih et al., 2013), board games (Silver et al., 2017), online multiplayer games (Berner et al., 2019) and imperfect-information games (Brown et al., 2020). These successes demonstrated RL’s ability to operate on ambiguous data, understand complex environments and infer high-level causal relationships. We believe these to be very relevant attributes for the application to biomedical KGs and drug discovery recommendations in general.

The approach of using RL for recommendation systems is increasing in popularity in industry and

academia (Afsar et al., 2021; Chen et al., 2019). RL has already been applied to the tasks of question answering (Das et al., 2018), fact-checking (Xiong et al., 2017) and recommendations (Liu et al., 2021).

Most of the approaches use path based RL reasoning, which sequentially traverses triples in a graph to make predictions. Because of this, it provides transparent reasoning for every prediction. An issue with this approach can be convergence and generating relevant reasoning paths. To help, demonstrations of reasoning can be provided by metapaths which acts as a form of weak supervision (Zhao et al., 2020; Liu et al., 2021). RL reasoning applied to the standard benchmarks graphs used in research has not shown promising performance and thus has not been the focus of much research. A small sample of path-based models and their characteristics are shown in Table 1.

MINERVA is a path based RL algorithm for the similar task of question answering. Two extensions of MINERVA, R2D2 and PoLo, applied the method to a biomedical KG (Hildebrandt et al., 2020; Liu et al., 2021). PoLo highlighted the potential for multi-hop reasoning to be especially suited to biomedical KGs.

Whilst promising in their approach, these works used Hetionet which is a relatively small KG that lacks the full complexity, size and noise found in industrial biomedical KGs. Additionally, Hetionet has not been updated since 2017. PoLo’s results came from testing a limited number (151) of Compound-treats-Disease links and the evaluation strategy was not standardised as pruning was not tested across all models. The ambiguity of how metrics are calculated also creates the possibility for unfair comparisons (Sun et al., 2020; Berrendorf et al., 2021). To overcome the limitations of these studies, we extend their work to larger biomedical KGs and offer a set of standardised evaluations.

3. Preliminaries

The algorithms MINERVA and PoLo are used for path-based RL reasoning to directly build on the claims in Liu et al. (2021) that the approach is suited to biomedical KGs. Both algorithms use the same definitions of the knowledge graph environment and task, which are defined below.

3.1. Knowledge Graph

A triple links two entities together. It is defined by (h, r, t) where h is the head entity, r is the relation, and t is the tail entity. An example of a triple would be $(Ibuprofen, treats, Headache)$. \mathcal{E} represents the full set of entities and \mathcal{R} the set full of relations in a graph. Every entity has a unique type \mathcal{T} . The KG is defined as a set of (h, r, t) triples $\mathcal{KG} \subset \mathcal{E} \times \mathcal{R} \times \mathcal{E}$. To enable RL agents to travel bidirectionally across triples, the inverse triples are added to the KG. The inverse relations are denoted as r^{-1} . For example for (e_1, r, e_2) the triple (e_2, r^{-1}, e_1) is also added. All triples in the KG are treated as true facts.

3.2. Metapaths

A metapath is a logical reasoning rule defining a general pathway between two entities. For example, a desired metapath for predicting $(Compound, treats, Disease)$ triples might be:

$$(Compound \xrightarrow{binds} Gene \xrightarrow{associates} Disease)$$

3.3. Recommendation

The task of recommendation is posed as a link prediction problem via sequential graph traversal. Given a query $(e_1, r, ?)$, such as $(COVID-19, treated\ by, ?)$, the task is to sequentially traverse triples in the KG to find the correct answer entities. At each step s in the graph, the set of possible actions is the outgoing triples of the current entity e_s . Each action is represented by the triples relation and tail entity (r, t) . Vector space embeddings are used to represent the relations and entities for input to the models. A 'NO_OP' action is augmented to each node, which effectively allows for no action to be taken and staying at the current node. A maximum number of steps is set to prevent the model from traversing indefinitely.

4. Experiments

We ran multiple experiments to establish if the path based RL reasoning approach is suited to biomedical recommendation tasks. We applied it to three different KGs on two separate tasks to draw concrete conclusions on its suitability. Ablations are performed to understand the approach in more depth.

Table 1: Sample of RL reasoning algorithms

Algorithm	Reference	Approach
DeepPath	Xiong et al. (2017)	RL path finding for fact checking
MINERVA	Das et al. (2018)	Policy-based RL for QA
M-Walk	Shen et al. (2018)	Monte Carlo Tree Search when sampling
MultiHop	Lin et al. (2018)	Soft reward and action dropout for MINERVA
PGPR	Xian et al. (2019)	Policy-based RL walks
RuleGuider	Lei et al. (2020)	Discovers rules to use for RL walks
R2D2	Hildebrandt et al. (2020)	MINERVA with debate dynamics
PoLo	Liu et al. (2021)	MINERVA with metapaths

4.1. Tasks

The models are evaluated on two common biomedical recommendation tasks: *drug repurposing* and *drug-target interaction*. In the first task, the goal is to find (*Compound, treats, Disease*) triples. Formally the query is defined as (*Compound, treats, ?*). For the second task, the goal is predicting (*Compound, binds, Gene*) triples, with the formal query being defined as (*Compound, binds, ?*).

4.2. Datasets

Three datasets are used. Hetionet as a small open-source baseline graph and two projections of Biological Insights Knowledge Graph (BIKG) (Geleta et al., 2021). BIKG is an internal biomedical KG actively used by *organization name anonymised for peer review* for recommendations. The two projections are ‘BIKG Hetionet’ and ‘BIKG Hetionet+’. The specific projections of BIKG are chosen as they represent the two separate structural types of biomedical KGs, which can be seen in Figure 4. Importantly, these specific datasets were chosen as they share the same core ontology as Hetionet (Figure 3), which allows for a unique systematic analysis.

Hetionet Hetionet (Himmelstein et al., 2017) is an open-source dataset developed in 2017 as part of a study looking at drug repurposing using a KG. It is the most commonly used biomedical graph for benchmarking. Hetionet combines data from 29 public databases and contains over 47k entities of 11 types, including genes, compounds and diseases. These are linked by over 2.2M edges of 24 different relation types. The full ontology is shown in Figure 3.

BIKG Hetionet BIKG (Geleta et al., 2021) unifies data from different public, private and internal sources into a single, comprehensive knowledge graph. BIKG Hetionet is a projection of BIKG using

the same Hetionet schema in Figure 3, except with almost five times more edges and three times more nodes. It represents the type of biomedical graph with a higher density and average degree (Figure 4). Usually this is because they do not include edges mined from literature. Exact dataset statistics can be found in Appendix A.

BIKG Hetionet+ Like other biomedical KGs, a large part of the full BIKG is from Natural Language Processing (NLP) pipelines which extract triples from literature. These are inherently more noisy and ambiguous edges. BIKG Hetionet+ extends on BIKG Hetionet by adding ‘has link’ NLP edges and 22 other new edge types. This nearly doubles the number of edge types. One extra node type ‘Mechanism of Action’ is also added. These additions result in a much noisier and more complex KG, representing the sparser biomedical graphs that contain literature edges and a lower average degree caused by a longer tail of poorly connected entities (Figure 4). Exact statistics can be found in Appendix A.

4.3. Algorithms

For the RL algorithm, MINERVA (Das et al., 2018) is selected. PoLo (Liu et al., 2021), which extends MINERVA with extra rewards for following pre-defined metapaths, is also used on the drug repurposing task. Using PoLo tests the effect of weak supervision from injecting prior domain knowledge. The metapaths are re-used from the original paper.

The following baseline algorithms were chosen to cover the different theoretical approaches and the most competitive models from the initial Liu et al. (2021) results on Hetionet – TransE (Wang et al., 2014), DistMult (Yang et al., 2014), R-GCN (Schlichtkrull et al., 2018) and AnyBURL (JUNO version) (Meilicke et al., 2019).

4.4. Evaluation Strategy

Ambiguity exists in the evaluation of link prediction methods. Metrics are not uniformly calculated across individual algorithm implementations and common software libraries. This leads to unfair comparisons in reported results (Sun et al., 2020; Berrendorf et al., 2021). Therefore, we implement a independent and standardised approach to fairly evaluate predictions. To the best of our knowledge, this is the first time it has been done for biomedical KG recommendations across symbolic, neural and neuro-symbolic methods.

All metrics are filtered (Bordes et al., 2013), deduplicated and evaluated for tail-sided predictions against all nodes in the graph. Pruning is also applied which filters predictions to only nodes of the correct target type, as this would be done before giving recommendation lists to scientists. Standard metrics for recommendation tasks are used, HITS@1, HITS@3, HITS@10, and mean reciprocal rank (MRR).

An initial hyperparameter search is applied for every dataset, task and model to find sensible hyperparameters (Appendix A). The best hyperparameters are used for training 5-fold cross-validation with seeded randomly split triples. Finally, the mean of the five runs is reported alongside standard errors.

5. Results

The results are shown in Table 2. The interpretable RL methods, MINERVA and PoLo, performed the best. Averaged across all datasets and tasks, MINERVA outperformed the best baselines by 41.8% for HITS@1, 24.3% for HITS@3, 7.3% for HITS@10 and 13.5% for MRR. Generating a average performance gain of 21.7% across metrics.

When metapaths were used in PoLo, it improved MINERVA’s average performance by a further 4.4%. We found applying pruning to RL results was especially important; leading to significant performance boosts, as it effectively eliminates incomplete and failed walks from predictions (Appendix C for pruned).

The RL approaches superior performance notably decreased as the graphs complexity increased. Falling from 41.7% performance gain in BIKG Hetionet to just 6.8% gain in BIKG Hetionet+. The improvement from metapaths also degraded from 5.4% on BIKG Hetionet to 2.7% across metrics for BIKG Hetionet+ as the metapaths became less relevant for the expanded ontology.

The baseline neural and symbolic methods varied in performance, whereas neurosymbolic methods (MINERVA and PoLo) were able to perform consistently across datasets and tasks. The embedding models (TransE & DistMult) struggled with larger biomedical KGs. However, TransE performed notably well for drug-target interaction. R-GCN performed relatively consistently but achieved a middle-of-the-pack performance. Finally, AnyBURL was competitive on larger graphs with the higher ambiguity. The symbolic rules managed to cut through the noise and perform well. However, in other graphs AnyBURL’s rigid rules limited its expressiveness.

In summary, we found that neural methods were better suited to smaller, cleaner biomedical KGs and symbolic methods were suited to larger, noisy biomedical KGs. However the neurosymbolic methods were able to perform consistently well across both.

5.1. Ablations

Impact of Multi-Hop Reasoning An ablation was ran to isolate the impact of single-hop vector space reasoning vs multi-hop symbolic reasoning. It was found that using multi-hop symbolic reasoning had better performance (Table 3) This ablation boosted the performance of black-box TransE recommendations whilst also providing the much needed explanations. It highlights the potential for multi-hop reasoning to work synergistically with graph representations usually used for single-hop vector space predictions. Multi-hop reasoning algorithms such as MINERVA could be a way to add explainability on top of black-box approaches like GNNs and traditional embeddings without sacrificing performance. However, further research is required into the extent that this is true.

Impact of Neural-Driven Reasoning A second ablation was run to see how the expressiveness of neural driven reasoning impacts performance. With superior symbolic rules as guidance, the extra expressiveness of neural-driven reasoning could not outperform the purely symbolic rules (Table 3). This shows how symbolic rules are very effective when there are high levels of noise and complexity in the KG. Even when being guided by the symbolic rules, the dynamic capability of the neural driven approach did not provide any benefits.

Table 2: Experiment results. **green** indicates the best result, **blue** indicates second best result. The interpretable, path based RL methods PoLo and MINERVA performed best.

Task	Dataset	Model	HITS@1	HITS@3	HITS@10	MRR
Drug Repurposing	Hetionet	TransE	.193 ± .027	.364 ± .031	.608 ± .034	.312 ± .022
		DistMult	.028 ± .002	.138 ± .022	.373 ± .039	.129 ± .002
		RGCN	.047 ± .028	.194 ± .018	.492 ± .043	.221 ± .040
		AnyBURL	.116 ± .013	.288 ± .024	.572 ± .036	.258 ± .012
		MINERVA	.351 ± .040	.559 ± .058	.790 ± .057	.463 ± .041
		PoLo	.378 ± .023	.575 ± .025	.845 ± .009	.479 ± .015
	BIKG Hetionet	TransE	.016 ± .003	.034 ± .005	.088 ± .001	.045 ± .004
		DistMult	.004 ± .002	.013 ± .002	.036 ± .007	.024 ± .003
		RGCN	.056 ± .005	.108 ± .008	.239 ± .008	.117 ± .005
		AnyBURL	.000 ± .000	.015 ± .001	.046 ± .004	.023 ± .001
		MINERVA	.121 ± .002	.194 ± .010	.249 ± .013	.160 ± .004
		PoLo	.124 ± .005	.204 ± .010	.273 ± .016	.167 ± .008
	BIKG Hetionet+	TransE	.017 ± .002	.052 ± .004	.119 ± .011	.057 ± .002
		DistMult	.004 ± .002	.014 ± .004	.039 ± .001	.026 ± .004
		RGCN	.039 ± .008	.104 ± .016	.222 ± .015	.115 ± .005
		AnyBURL	.000 ± .000	.056 ± .006	.205 ± .014	.072 ± .002
		MINERVA	.076 ± .008	.124 ± .011	.166 ± .013	.113 ± .010
		PoLo	.074 ± .006	.133 ± .010	.173 ± .012	.115 ± .007
Drug-Target Interaction	Hetionet	TransE	.287 ± .008	.546 ± .013	.918 ± .007	.331 ± .005
		DistMult	.039 ± .004	.128 ± .007	.367 ± .012	.115 ± .005
		RGCN	.060 ± .025	.177 ± .057	.376 ± .102	.126 ± .031
		AnyBURL	.169 ± .043	.323 ± .081	.493 ± .124	.210 ± .051
		MINERVA	.186 ± .015	.420 ± .028	.807 ± .039	.296 ± .019
		BIKG Hetionet	TransE	.193 ± .001	.376 ± .012	.674 ± .012
	DistMult	.044 ± .007	.111 ± .014	.269 ± .014	.098 ± .007	
	RGCN	.173 ± .016	.338 ± .013	.539 ± .021	.235 ± .008	
	AnyBURL	.215 ± .005	.408 ± .004	.623 ± .009	.264 ± .004	
	MINERVA	.235 ± .005	.516 ± .011	.983 ± .015	.305 ± .004	
	BIKG Hetionet+	TransE	.054 ± .004	.098 ± .007	.171 ± .011	.008 ± .004
		DistMult	.035 ± .006	.084 ± .011	.206 ± .029	.084 ± .001
		RGCN	.188 ± .008	.323 ± .019	.539 ± .010	.241 ± .006
		AnyBURL	.215 ± .003	.408 ± .008	.622 ± .005	.263 ± .003
		MINERVA	.181 ± .006	.368 ± .008	.628 ± .019	.243 ± .004
		PoLo	.191 ± .009	.366 ± .012	.596 ± .019	.250 ± .010

Table 3: *Multi-Hop Ablation*. Retraining MINERVA using the same embeddings from TransE where they initially performed best (Drug-Target Interaction on Hetionet) improved performance. *Neural-Driven Ablation*. Where AnyBURLs symbolic rules performed best (Drug-Target Interaction on BIKG Hetionet+) the same rules were reused as metapaths in PoLo but it failed to improve performance.

Ablation	Model	HITS@1	HITS@3	HITS@10	MRR
Multi-Hop	TransE	.287 ± .008	.546 ± .013	.918 ± .007	.331 ± .005
	MINERVA	.186 ± .015	.420 ± .028	.807 ± .039	.296 ± .019
	MINERVA*	.327 ± .014	.622 ± .013	.938 ± .018	.350 ± .006
Neural-Driven	AnyBURL	.215 ± .003	.408 ± .008	.622 ± .005	.263 ± .003
	MINERVA	.181 ± .006	.368 ± .008	.628 ± .019	.243 ± .004
	PoLo*	.191 ± .009	.366 ± .012	.596 ± .019	.250 ± .010

6. Explanations

Although the results are promising, Lv et al. (2021) claim the reasoning produced by multi-hop models can have gaps in interpretability. If the explanations are unclear to the end user, it will be detrimental to trust. To address this aspect, we run inference on the full BIKG Hetionet and BIKG Hetionet+ graphs, using the trained MINERVA models. We then assess the resulting high-level metapaths and individual reasoning paths for biological relevance.

6.1. Reasoning Metapaths

We found that the high-level metapaths displayed sensible biological logic. The reasoning ranges from clear interactions between genes, mechanisms of action and biological pathways to more vague similarity-based reasons such as compounds that resemble each other (Figure 5 & 6). However, inspection of the metapaths also revealed that models can get fixated on less successful policies, almost exclusively focusing on mechanisms of action entities in BIKG Hetionet+ and using more cyclic paths, which ultimately led to lower performance. The top 10 metapaths and their frequency can be found in Appendix B.

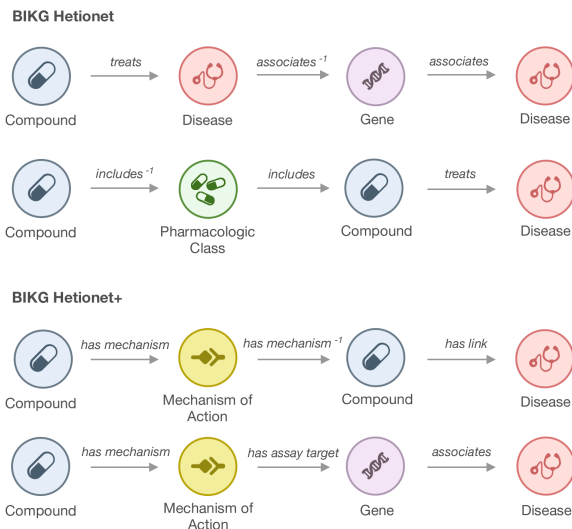


Figure 5: MINERVA’s most common metapaths for drug repurposing

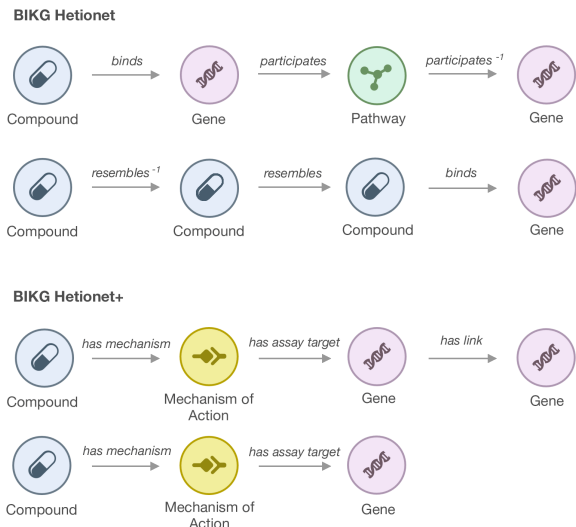


Figure 6: MINERVA’s most common metapaths for drug-target interaction

6.2. Case Studies

Although the high-level metapaths appear to be relevant, the low-level reasoning could still be biologically flawed. Therefore, together with subject matter experts we investigated a sample of the individual reasoning paths to check the validity.

Novel predictions were made for Lixisenatide, Dulafutide and similar compounds to treat non-alcoholic fatty liver disease (NAFLD). It was able to correctly reason that they act as a receptor agonist (RA) for the gene Glucagon-like peptide-1 receptor (GLP1R). There is literature supporting the role of GLP-1 RA’s as a treatment for NAFLD (Seghieri et al., 2018; Lv et al., 2020), as well as clinical trials and case studies for NAFLD treatment (Gluud et al., 2014; Seko et al., 2017). The next highest prediction for NAFLD was for Secukinumab, which follows a similar reasoning but instead via Interleukin-17A inhibition. There is a clinical trial currently recruiting to study this on ClinicalTrials.gov (NCT04237116).

Everolimus, usually used to treat cancer, was unconventionally predicted to treat unipolar depression (Figure 1). However there is case study evidence to support this theory (Mir et al., 2018). The reasoning was due to links with Cytochrome P450, which has known links to depression via the mTor pathway. It also links to Gene PLXNA3, which is important

for neurological development and has studies linking it to depression (Wray et al., 2007). This is a more speculative, but still biologically relevant, reasoning that would require additional validation work from drug discovery scientists.

Finally, a prediction was made of Simvastatin binding to gene UGT1A1. This example highlights how the predictions and explanations are susceptible to errors in the KG data. The reasoning used the edges of Simvastatin binding to enzymatic genes CYP2D6, SLCO1B1 and CYP3A5, which are involved in drug metabolic pathways. UGT1A1 was also shown to be a participant in these pathways, and therefore it reasoned that Simvastatin was likely to bind to UGT1A1. All these enzymatic genes are indeed involved in Simvastatin metabolism (Iwuchukwu et al., 2014). However, they do not actually 'bind' to these genes, the edges are misclassified and should be 'affects'. The benefit of the transparent explanations is that a scientist can easily identify this fault and dismiss the recommendation. It also means data issues can easily be identified and fixed, which creates higher quality KG datasets. Whereas for black-box recommendations the fault in the reasoning would be invisible to end users and likely go unnoticed.

These case studies are typical of the types of biological reasoning that can be found throughout the predictions, with some novel and interesting explanations. There is also a proportion of predictions with more ambiguity, linking entities together via similar genes, compounds and pharmacological classes. We provide more examples in Appendix B.

7. Implications

The superior performance we observed and the accompanying transparent explanations make the RL approach well suited to biomedical recommendations. The general approach can be extended to produce even greater explanations. RL's reward function enables users to have more control over the reasoning used and it's possible to provide reasons a recommendation might not be true (Hildebrandt et al., 2020).

Additionally, the multi-hop approach allows for an interactive, human-in-the-loop reasoning process. Humans and AI can collaborate by combining knowledge to collaboratively walk across the knowledge graph to make predictions. All these attributes mean the approach can create better informed, more trusted biomedical recommendations without compromising on accuracy.

8. Conclusions

This paper highlights that biomedical KG recommendation is a unique challenge that cannot be approached in the same way as other recommendation tasks. The reality of the problem demands recommendations to be human-centric and it is shown that biomedical KGs unique structure differentiates them as a distinct problem. Different theoretical types of algorithms were evaluated across multiple representative datasets and tasks. It was found that multi-hop neural-driven symbolic reasoning, using RL, outperformed other approaches. Additionally, using this approach we were able to produce novel and relevant biological explanations. An ablation also highlighted the potential for this approach to create explanations for black-box models whilst boosting performance. Therefore, we believe the approach is well suited to biomedical recommendations and encourage more research in this direction.

Acknowledgments

The authors would like to thank Fatima Lugtu, Greet De Baets and Piotr Grabowski for their assistance in evaluating the recommendations and explanations. Thanks also goes to the SCP (Scientific Compute Platform) team at AstraZeneca.

References

- Martín Abadi, Paul Barham, Jianmin Chen, Zhifeng Chen, Andy Davis, Jeffrey Dean, Matthieu Devin, Sanjay Ghemawat, Geoffrey Irving, Michael Isard, et al. TensorFlow: A System for Large-Scale Machine Learning. In *12th {USENIX} Symposium on Operating Systems Design and Implementation ({OSDI} 16)*, pages 265–283, 2016.
- M Mehdi Afsar, Trafford Crump, and Behrouz Far. Reinforcement learning based recommender systems: A survey. *arXiv preprint arXiv:2101.06286*, 2021.
- Takuya Akiba, Shotaro Sano, Toshihiko Yanase, Takeru Ohta, and Masanori Koyama. Optuna: A next-generation hyperparameter optimization framework. In *Proceedings of the 25th ACM SIGKDD International Conference on Knowledge Discovery & Data mining*, pages 2623–2631, 2019.
- David Austin and Tamara Hayford. Research and development in the pharmaceutical industry, Apr 2021. URL <https://www.cbo.gov/publication/57025>.
- Albert-László Barabási, Natali Gulbahce, and Joseph Loscalzo. Network Medicine: a Network-based Approach to Human Disease. *Nature Reviews Genetics*, 12(1):56–68, 2011.
- Christopher Berner, Greg Brockman, Brooke Chan, Vicki Cheung, Przemysław Debiak, Christy Dennison, David Farhi, Quirin Fischer, Shariq Hashme, Chris Hesse, et al. Dota 2 with large scale deep reinforcement learning. *arXiv preprint arXiv:1912.06680*, 2019.
- Max Berrendorf, Evgeniy Faerman, Laurent Vermue, and Volker Tresp. On the Ambiguity of Rank-Based Evaluation of Entity Alignment or Link Prediction Methods, 2021.
- Stephen Bonner, Ian P Barrett, Cheng Ye, Rowan Swiers, Ola Engkvist, Andreas Bender, Charles Tappley Hoyt, and William Hamilton. A review of biomedical datasets relating to drug discovery: A knowledge graph perspective, 2021.
- Antoine Bordes, Nicolas Usunier, Alberto Garcia-Duran, Jason Weston, and Oksana Yakhnenko. Translating Embeddings for Modeling Multi-relational Data. In C. J. C. Burges, L. Bottou, M. Welling, Z. Ghahramani, and K. Q. Weinberger, editors, *Advances in Neural Information Processing Systems*, volume 26. Curran Associates, Inc., 2013.
- Anna Breit, Simon Ott, Asan Agibetov, and Matthias Samwald. OpenBioLink: A Benchmarking Framework for Large-Scale Biomedical Link Prediction. *Bioinformatics*, 36(13):4097–4098, 2020.
- Noam Brown, Anton Bakhtin, Adam Lerer, and Qucheng Gong. Combining deep reinforcement learning and search for imperfect-information games. *arXiv preprint arXiv:2007.13544*, 2020.
- Minmin Chen, Alex Beutel, Paul Covington, Sagar Jain, Francois Belletti, and Ed H Chi. Top-k off-policy correction for a reinforce recommender system. In *Proceedings of the Twelfth ACM International Conference on Web Search and Data Mining*, pages 456–464, 2019.
- Feixiong Cheng, István A Kovács, and Albert-László Barabási. Network-based Prediction of Drug Combinations. *Nature Communications*, 10(1):1–11, 2019.
- Rajarshi Das, Shehzaad Dhuliawala, Manzil Zaheer, Luke Vilnis, Ishan Durugkar, Akshay Krishnamurthy, Alex Smola, and Andrew McCallum. Go for a Walk and Arrive at the Answer: Reasoning Over Paths in Knowledge Bases Using Reinforcement Learning. In *International Conference on Learning Representations*, 2018. URL <https://openreview.net/forum?id=Syg-YfWCW>.
- Tim Dettmers, Pasquale Minervini, Pontus Stenertorp, and Sebastian Riedel. Convolutional 2D Knowledge Graph Embeddings. In *Thirty-Second AAAI Conference on Artificial Intelligence*, 2018.
- Matthias Fey and Jan Eric Lenssen. Fast graph representation learning with PyTorch Geometric. *arXiv preprint arXiv:1903.02428*, 2019.

- David Geleta, Andriy Nikolov, Gavin Edwards, Anna Gogleva, Richard Jackson, Erik Jansson, Andrej Lamov, Sebastian Nilsson, Marina Pettersson, Vladimir Poroshin, Benedek Rozemberczki, Timothy Scrivener, Michael Ughetto, and Eliseo Papa. Biological insights knowledge graph: an integrated knowledge graph to support drug development, 2021. URL <https://doi.org/10.1101/2021.10.28.466262>.
- Lise L Gluud, Filip K Knop, and Tina Vilsbøll. Effects of lixisenatide on elevated liver transaminases: systematic review with individual patient data meta-analysis of randomised controlled trials on patients with type 2 diabetes. *BMJ open*, 4(12): e005325, 2014.
- Anna Gogleva, Dimitris Polychronopoulos, Matthias Pfeifer, Vladimir Poroshin, Michaël Ughetto, Ben Sidders, Jonathan Dry, Miika Ahdesmäki, Ultan McDermott, Eliseo Papa, et al. Knowledge graph-based recommendation framework identifies novel drivers of resistance in egfr mutant non-small cell lung cancer. *bioRxiv*, 2021.
- Lingbing Guo, Zequn Sun, and Wei Hu. Learning to exploit long-term relational dependencies in knowledge graphs. In *International Conference on Machine Learning*, pages 2505–2514. PMLR, 2019.
- Deisy Morselli Gysi, Ítalo Do Valle, Marinka Zitnik, Asher Ameli, Xiao Gan, Onur Varol, Susan Dina Ghiassian, JJ Patten, Robert A Davey, Joseph Loscalzo, et al. Network Medicine Framework for Identifying Drug-Repurposing Opportunities for COVID-19. *Proceedings of the National Academy of Sciences*, 118(19), 2021.
- John Haugeland. *Artificial intelligence: The very idea*. MIT press, 1989.
- Marcel Hildebrandt, Jorge Andres Quintero Serna, Yunpu Ma, Martin Ringsquandl, Mitchell Joblin, and Volker Tresp. Reasoning on knowledge graphs with debate dynamics. In *Proceedings of the AAAI Conference on Artificial Intelligence*, volume 34, pages 4123–4131, 2020.
- Daniel Scott Himmelstein, Antoine Lizee, Christine Hessler, Leo Brueggeman, Sabrina L Chen, Dexter Hadley, Ari Green, Pouya Khankhanian, and Sergio E Baranzini. Systematic Integration of Biomedical Knowledge Prioritizes Drugs for Repurposing. *Elife*, 6:e26726, 2017.
- Weihua Hu, Matthias Fey, Marinka Zitnik, Yuxiao Dong, Hongyu Ren, Bowen Liu, Michele Catasta, and Jure Leskovec. Open Graph Benchmark: Datasets for Machine Learning on Graphs. *arXiv preprint arXiv:2005.00687*, 2020.
- Vassilis N Ioannidis, Xiang Song, Saurav Manchanda, Mufei Li, Xiaoqin Pan, Da Zheng, Xia Ning, Xiangxiang Zeng, and George Karypis. DRKG - Drug Repurposing Knowledge Graph for COVID-19, 2020.
- Otito F Iwuchukwu, QiPing Feng, Wei-Qi Wei, Lan Jiang, Min Jiang, Hua Xu, Joshua C Denny, Russell A Wilke, Ronald M Krauss, Dan M Roden, et al. Genetic variation in the ugt1a locus is associated with simvastatin efficacy in a clinical practice setting. *Pharmacogenomics*, 15(14):1739–1747, 2014.
- Diederik P. Kingma and Jimmy Ba. Adam: A method for stochastic optimization, 2017.
- Thomas N Kipf and Max Welling. Semi-supervised classification with graph convolutional networks. *arXiv preprint arXiv:1609.02907*, 2016.
- Deren Lei, Gangrong Jiang, Xiaotao Gu, Kexuan Sun, Yuning Mao, and Xiang Ren. Learning Collaborative Agents with Rule Guidance for Knowledge Graph Reasoning. In *Proceedings of the 2020 Conference on Empirical Methods in Natural Language Processing (EMNLP)*, pages 8541–8547, 2020.
- Xi Victoria Lin, Richard Socher, and Caiming Xiong. Multi-hop knowledge graph reasoning with reward shaping. *arXiv preprint arXiv:1808.10568*, 2018.
- Yushan Liu, Marcel Hildebrandt, Mitchell Joblin, Martin Ringsquandl, Rime Raissouni, and Volker Tresp. Neural Multi-Hop Reasoning With Logical Rules on Biomedical Knowledge Graphs. In *European Semantic Web Conference*, pages 375–391. Springer, 2021.
- Xiaodan Lv, Yongqiang Dong, Lingling Hu, Feiyu Lu, Changyu Zhou, and Shaoyou Qin. Glucagon-like peptide-1 receptor agonists (glp-1 ras) for the management of nonalcoholic fatty liver disease (nafld): A systematic review. *Endocrinology, diabetes & metabolism*, 3(3):e00163, 2020.

- Xin Lv, Yixin Cao, Lei Hou, Juanzi Li, Zhiyuan Liu, Yichi Zhang, and Zelin Dai. Is multi-hop reasoning really explainable? towards benchmarking reasoning interpretability. *arXiv preprint arXiv:2104.06751*, 2021.
- Christian Meilicke, Melisachew Wudage Chekol, Daniel Ruffinelli, and Heiner Stuckenschmidt. Anytime Bottom-Up Rule Learning for Knowledge Graph Completion. In *IJCAI*, pages 3137–3143, 2019.
- Olivier Mir, Alexandre Salvador, Sarah Dauchy, Stanislas Ropert, Cédric Lemogne, and Raphaël Gaillard. Everolimus induced mood changes in breast cancer patients: a case-control study. *Investigational new drugs*, 36(3):503–508, 2018.
- Volodymyr Mnih, Koray Kavukcuoglu, David Silver, Alex Graves, Ioannis Antonoglou, Daan Wierstra, and Martin Riedmiller. Playing atari with deep reinforcement learning. *arXiv preprint arXiv:1312.5602*, 2013.
- Vinod Nair and Geoffrey E Hinton. Rectified linear units improve restricted boltzmann machines. In *Icml*, 2010.
- Adam Paszke, Sam Gross, Soumith Chintala, Gregory Chanan, Edward Yang, Zachary DeVito, Zeming Lin, Alban Desmaison, Luca Antiga, and Adam Lerer. Automatic differentiation in pytorch. *NIPS*, 2017.
- Meng Qu and Jian Tang. Probabilistic logic neural networks for reasoning. *arXiv preprint arXiv:1906.08495*, 2019.
- Tim Rocktäschel and Sebastian Riedel. End-to-end differentiable proving. *arXiv preprint arXiv:1705.11040*, 2017.
- Frank Rosenblatt. The perceptron: a probabilistic model for information storage and organization in the brain. *Psychological review*, 65(6):386, 1958.
- David E Rumelhart, Geoffrey E Hinton, and Ronald J Williams. Learning representations by back-propagating errors. *nature*, 323(6088):533–536, 1986.
- Alberto Santos, Ana Rita Colaço, Annelaura Bach Nielsen, Lili Niu, Philipp Emanuel Geyer, Fabian Coscia, Nicolai Jacob Wewer Albrechtsen, Filip Mundt, Lars Juhl Jensen, and Matthias Mann. Clinical Knowledge Graph Integrates Proteomics Data Into Clinical Decision-Making. *bioRxiv*, 2020.
- Michael Schlichtkrull, Thomas N Kipf, Peter Bloem, Rianne Van Den Berg, Ivan Titov, and Max Welling. Modeling Relational Data with Graph Convolutional Networks. In *European Semantic Web Conference*, pages 593–607. Springer, 2018.
- Marta Seghieri, Alexander S Christensen, Andreas Andersen, Anna Solini, Filip K Knop, and Tina Vilsbøll. Future perspectives on glp-1 receptor agonists and glp-1/glucagon receptor co-agonists in the treatment of nafld. *Frontiers in endocrinology*, 9:649, 2018.
- Yuya Seko, Yoshio Sumida, Saiyu Tanaka, Kojiro Mori, Hiroyoshi Taketani, Hiroshi Ishiba, Tasuku Hara, Akira Okajima, Atsushi Umemura, Taichiro Nishikawa, et al. Effect of 12-week dulaglutide therapy in japanese patients with biopsy-proven non-alcoholic fatty liver disease and type 2 diabetes mellitus. *Hepatology Research*, 47(11):1206–1211, 2017.
- Yelong Shen, Jianshu Chen, Po-Sen Huang, Yuqing Guo, and Jianfeng Gao. M-Walk: Learning to Walk Over Graphs Using Monte Carlo Tree Search. In *Proceedings of the 32nd International Conference on Neural Information Processing Systems*, pages 6787–6798, 2018.
- David Silver, Julian Schrittwieser, Karen Simonyan, Ioannis Antonoglou, Aja Huang, Arthur Guez, Thomas Hubert, Lucas Baker, Matthew Lai, Adrian Bolton, et al. Mastering the game of go without human knowledge. *nature*, 550(7676):354–359, 2017.
- Nitish Srivastava, Geoffrey Hinton, Alex Krizhevsky, Ilya Sutskever, and Ruslan Salakhutdinov. Dropout: a simple way to prevent neural networks from overfitting. *The journal of machine learning research*, 15(1):1929–1958, 2014.
- Zhiqing Sun, Shikhar Vashishth, Soumya Sanyal, Partha Talukdar, and Yiming Yang. A Re-evaluation of Knowledge Graph Completion Methods, 2020.
- Kristina Toutanova, Danqi Chen, Patrick Pantel, Hoifung Poon, Pallavi Choudhury, and Michael Gamon. Representing Text for Joint Embedding of Text and Knowledge Bases. In *Proceedings of the*

- 2015 Conference on Empirical Methods in Natural Language Processing, pages 1499–1509, 2015.
- Brian Walsh, Sameh K Mohamed, and Vít Nováček. BioKG: A Knowledge Graph for Relational Learning On Biological Data. In *Proceedings of the 29th ACM International Conference on Information & Knowledge Management*, pages 3173–3180, 2020.
- Zhen Wang, Jianwen Zhang, Jianlin Feng, and Zheng Chen. Knowledge Graph Embedding by Translating on Hyperplanes. In *Proceedings of the AAAI Conference on Artificial Intelligence*, volume 28, 2014.
- Naomi R Wray, Michael R James, Steven P Mah, Matthew Nelson, Gavin Andrews, Patrick F Sullivan, Grant W Montgomery, Andrew J Birley, Andreas Braun, and Nicholas G Martin. Anxiety and comorbid measures associated with plxna2. *Archives of general psychiatry*, 64(3):318–326, 2007.
- Zonghan Wu, Shirui Pan, Fengwen Chen, Guodong Long, Chengqi Zhang, and S Yu Philip. A comprehensive survey on graph neural networks. *IEEE transactions on neural networks and learning systems*, 32(1):4–24, 2020.
- Yikun Xian, Zuohui Fu, Shan Muthukrishnan, Gerard De Melo, and Yongfeng Zhang. Reinforcement Knowledge Graph Reasoning for Explainable Recommendation. In *Proceedings of the 42nd International ACM SIGIR Conference on Research and Development in Information Retrieval*, pages 285–294, 2019.
- Wenhan Xiong, Thien Hoang, and William Yang Wang. DeepPath: A Reinforcement Learning Method for Knowledge Graph Reasoning. In *Proceedings of the 2017 Conference on Empirical Methods in Natural Language Processing*, pages 564–573, 2017.
- Bishan Yang, Wen-tau Yih, Xiaodong He, Jianfeng Gao, and Li Deng. Embedding entities and relations for learning and inference in knowledge bases. *arXiv preprint arXiv:1412.6575*, 2014.
- Fan Yang, Zhilin Yang, and William W Cohen. Differentiable learning of logical rules for knowledge base reasoning. *arXiv preprint arXiv:1702.08367*, 2017.
- Jing Zhang, Bo Chen, Lingxi Zhang, Xirui Ke, and Haipeng Ding. Neural, Symbolic and Neural-symbolic Reasoning on Knowledge Graphs. *AI Open*, 2:14–35, 2021.
- Kangzhi Zhao, Xiting Wang, Yuren Zhang, Li Zhao, Zheng Liu, Chunxiao Xing, and Xing Xie. Leveraging Demonstrations for Reinforcement Recommendation Reasoning Over Knowledge Graphs. In *Proceedings of the 43rd International ACM SIGIR Conference on Research and Development in Information Retrieval*, pages 239–248, 2020.
- Da Zheng, Xiang Song, Chao Ma, Zeyuan Tan, Zihao Ye, Jin Dong, Hao Xiong, Zheng Zhang, and George Karypis. DGL-KE: Training Knowledge Graph Embeddings at Scale. In *Proceedings of the 43rd International ACM SIGIR Conference on Research and Development in Information Retrieval*, pages 739–748, 2020a.
- Shuangjia Zheng, Jiahua Rao, Ying Song, Jixian Zhang, Xianglu Xiao, Evandro Fei Fang, Yuedong Yang, and Zhangming Niu. PharmKG: A Dedicated Knowledge Graph Benchmark for Biomedical Data Mining. *Briefings in Bioinformatics*, 2020b.
- Yadi Zhou, Yuan Hou, Jiayu Shen, Yin Huang, William Martin, and Feixiong Cheng. Network-based Drug Repurposing for Novel Coronavirus 2019-nCoV/SARS-CoV-2. *Cell Discovery*, 6(1):1–18, 2020.

Appendix A. Experimental Details

A.1. Model Implementations

Our experiments with PoLo and MINERVA utilized the TensorFlow (Abadi et al., 2016) codebase released by the authors of PoLo. AnyBURL (Meilicke et al., 2019) uses the latest version (AnyBURL-JUNO) from the authors. The DistMult and TransE (L2 norm) embeddings were learned with the DGL-KE (Zheng et al., 2020a) on top of the PyTorch (Paszke et al., 2017) automatic differentiation backend library. The hyperparameters of these embedding models were tuned on the validation set with the open-source Optuna framework (Akiba et al., 2019). Finally, the R-GCN baselines were generated with the PyTorch Geometric library (Fey and Lenssen, 2019) using Adam optimiser Kingma and Ba (2017), Dropout Srivastava et al. (2014) and ReLU Nair and Hinton (2010).

A.2. Hyperparameters

To get the best results for each model, the Table X and Y show hyperparameters that are searched. For MINERVA, λ is set to 0 which recovers MINERVA from PoLo.

Table 4: Hyperparameter search space for MINERVA and PoLo. For MINERVA λ is set to 0.

Hyperparameter	Values
Embedding size	{128, 256}
Hidden layer size	{256,512}
Learning rate	{0.0001,0.001}
λ	{0.1,1}
β	{0.01,0.1}

Table 5: Hyperparameter search space for knowledge graph embedding techniques TransE and DistMult.

Hyperparameter	Values
Embedding size	{128, 256, ..., 1024}
Learning rate	[0.001,0.2]
Negative samples	{1,...,500}
Max step	{12000, 22000, ..., 200000}

Table 6: Hyperparameter search space for R-GCN.

Hyperparameter	Values
Embedding size	{32, 64, 128}
Learning rate	{0.01, 0.05}
Negative samples	{10}
Max step	{0.01}

AnyBURL We use the most recent (JUNO) version of AnyBURL, which is more of a neurosymbolic approach as it implements Reinforcement Learning to learn rules. The maximum length of rules is set to 3 and the rules are learned for a total of 500 seconds. The AnyBURL algorithm does not need hyperparameter tuning to achieve good results, therefore we kept the default values of remaining hyperparameters.

A.3. Dataset Statistics

Table 7: Statistics of each tasks dataset sizes

Task	Dataset	Relation	Nodes	Edges	Train	Valid	Test
Drug Repurposing	Hetionet	CtD	47,031	2,250,197	483	121	151
	BIKG Hetionet	CtD	131,668	11,289,713	2,062	516	664
	BIKG Hetionet+	CtD	556,219	25,762,310	2,114	529	661
Drug-Target Interaction	Hetionet	CbG	47,031	2,250,197	7,404	1,852	2,315
	BIKG Hetionet	CbG	131,668	11,289,713	7,351	1,838	2,298
	BIKG Hetionet+	CbG	556,219	25,762,310	7,351	1,838	2,298

Table 8: Statistics of biomedical and benchmark knowledge graphs

Dataset	Domain	Node Types	Nodes	Edge Types	Edges	Mean Degree
ClinicalKG	Biological	35	19,251,579	57	208,177,953	21.63
BIKG	Biological	27	10,948,027	52	83,849,252	17.87
BIKG Hetionet+	Biological	12	556,219	47	25,762,310	92.63
BIKG Hetionet	Biological	11	131,668	24	11,289,713	171.49
DRKG	Biological	13	97,238	107	5,874,258	120.81
OGBL-BIOKG	Biological	5	45,085	51	4,762,677	108.52
OpenBioLink-HQ	Biological	7	184,667	30	4,778,683	51.80
Hetionet	Biological	11	47,031	24	2,250,197	95.83
BioKG	Biological	10	105,524	17	2,067,998	39.19
PharmKG-8k	Biological	3	7,262	29	479,902	132.16
FB15K-237	General	571	14,505	237	310,116	42.50
WN18RR	Lexical	4	40,945	11	90,003	4.53
NELL-995	General	269	75,492	200	154,213	4.09

Appendix B. Explanations

The following section contains metapath statistics and explanations generated by MINVERA on the BIKG Hetionet and BIKG Hetionet+ datasets.

B.1. Metapaths Statistics

Table 9: MINVERA’s top 10 frequent reasoning metapaths for drug repurposing (pruned)

Dataset	Metapath	%
BIKG Hetionet	$Compound \xrightarrow{\text{treats}} Disease \xrightarrow{\text{associates}^{-1}} Gene \xrightarrow{\text{associates}} Disease$	71.7
	$Compound \xrightarrow{\text{includes}^{-1}} Pharmacologic\ Class \xrightarrow{\text{includes}} Compound \xrightarrow{\text{treats}} Disease$	5.1
	$Compound \xrightarrow{\text{treats}} Disease \xrightarrow{\text{upregulates}} Gene \xrightarrow{\text{associates}} Disease$	4.3
	$Compound \xrightarrow{\text{treats}} Disease \xrightarrow{\text{treats}^{-1}} Compound \xrightarrow{\text{treats}} Disease$	2.7
	$Compound \xrightarrow{\text{palliates}} Disease \xrightarrow{\text{upregulates}} Gene \xrightarrow{\text{associates}} Disease$	2.1
	$Compound \xrightarrow{\text{resembles}} Compound \xrightarrow{\text{resembles}} Compound \xrightarrow{\text{treats}} Disease$	1.5
	$Compound \xrightarrow{\text{binds}} Gene \xrightarrow{\text{associates}} Disease$	1.2
	$Compound \xrightarrow{\text{resembles}} Compound \xrightarrow{\text{resembles}^{-1}} Compound \xrightarrow{\text{treats}} Disease$	1.2
	$Compound \xrightarrow{\text{palliates}} Disease \xrightarrow{\text{associates}^{-1}} Gene \xrightarrow{\text{associates}} Disease$	1.2
	$Compound \xrightarrow{\text{treats}} Disease \xrightarrow{\text{localizes}} Anatomy \xrightarrow{\text{localizes}^{-1}} Disease'$	0.9
BIKG Hetionet+	$Compound \xrightarrow{\text{has mechanism}} Mechanism\ of\ Action \xrightarrow{\text{has mechanism}^{-1}} Compound \xrightarrow{\text{has link}} Disease$	51.5
	$Compound \xrightarrow{\text{has mechanism}} Mechanism\ of\ Action \xrightarrow{\text{has assay target}} Gene \xrightarrow{\text{associates}} Disease$	34.2
	$Compound \xrightarrow{\text{has link}} Disease \xrightarrow{\text{has link}^{-1}} Disease \xrightarrow{\text{has link}} Disease$	9.2
	$Compound \xrightarrow{\text{has mechanism}} Mechanism\ of\ Action \xrightarrow{\text{has assay target}} Gene \xrightarrow{\text{has link}} Disease$	1.6
	$Compound \xrightarrow{\text{treats}} Disease \xrightarrow{\text{has link}^{-1}} Compound \xrightarrow{\text{has link}} Disease$	1.3
	$Compound \xrightarrow{\text{treats}} Disease \xrightarrow{\text{associates}^{-1}} Gene \xrightarrow{\text{associates}} Disease$	0.4
	$Compound \xrightarrow{\text{resembles}} Compound \xrightarrow{\text{binds}} Gene \xrightarrow{\text{associates}} Disease$	0.3
	$Compound \xrightarrow{\text{has link}} Disease \xrightarrow{\text{involved in}^{-1}} Biological\ Process \xrightarrow{\text{involved in}} Disease$	0.2
	$Compound \xrightarrow{\text{resembles}^{-1}} Compound \xrightarrow{\text{binds}} Gene \xrightarrow{\text{associates}} Disease$	0.2
	$Compound \xrightarrow{\text{treats}} Disease \xrightarrow{\text{involved in}^{-1}} Biological\ Process \xrightarrow{\text{involved in}} Disease$	0.1

Table 10: MINERVA’s top 10 frequent reasoning metapaths for drug target interaction (pruned)

Dataset	Metapath	%
BIKG Hetionet	$Compound \xrightarrow{\text{binds}} Gene \xrightarrow{\text{participates}} Pathway \xrightarrow{\text{participates}^{-1}} Gene$	14.2
	$Compound \xrightarrow{\text{resembles}^{-1}} Compound \xrightarrow{\text{resembles}} Compound \xrightarrow{\text{binds}} Gene$	13.8
	$Compound \xrightarrow{\text{includes}^{-1}} Pharmacologic\ Class \xrightarrow{\text{includes}} Compound \xrightarrow{\text{binds}} Gene$	13.2
	$Compound \xrightarrow{\text{resembles}} Compound \xrightarrow{\text{resembles}} Compound \xrightarrow{\text{binds}} Gene$	12.4
	$Compound \xrightarrow{\text{resembles}} Compound \xrightarrow{\text{resembles}^{-1}} Compound \xrightarrow{\text{binds}} Gene$	12.2
	$Compound \xrightarrow{\text{binds}} Gene \xrightarrow{\text{participates}} Molecular\ Function \xrightarrow{\text{participates}^{-1}} Gene$	4.8
	$Compound \xrightarrow{\text{resembles}} Compound \xrightarrow{\text{binds}} Gene$	3.5
	$Compound \xrightarrow{\text{resembles}} Compound \xrightarrow{\text{binds}} Gene$	3.3
	$Compound \xrightarrow{\text{binds}} Gene \xrightarrow{\text{participates}} Biological\ Process \xrightarrow{\text{participates}} Gene$	3.2
	$Compound \xrightarrow{\text{resembles}^{-1}} Compound \xrightarrow{\text{resembles}^{-1}} Compound \xrightarrow{\text{binds}} Gene$	3.2
BIKG Hetionet+	$Compound \xrightarrow{\text{has mechanism}} Mechanism\ of\ Action \xrightarrow{\text{has assay target}} Gene \xrightarrow{\text{has link}} Gene$	47.6
	$Compound \xrightarrow{\text{has mechanism}} Mechanism\ of\ Action \xrightarrow{\text{has assay target}} Gene$	18.8
	$Compound \xrightarrow{\text{has mechanism}} Mechanism\ of\ Action \xrightarrow{\text{has assay target}} Gene \xrightarrow{\text{interacts}} Gene$	10.1
	$Compound \xrightarrow{\text{binds}} Gene \xrightarrow{\text{has link}} Gene \xrightarrow{\text{has link}} Gene$	5.9
	$Compound \xrightarrow{\text{has link}} Gene \xrightarrow{\text{has link}} Gene \xrightarrow{\text{has link}} Gene$	3.0
	$Compound \xrightarrow{\text{binds}} Gene \xrightarrow{\text{has link}} Gene$	2.2
	$Compound \xrightarrow{\text{associates}} Pathway \xrightarrow{\text{involved in}} Disease \xrightarrow{\text{associates}^{-1}} Gene$	1.4
	$Compound \xrightarrow{\text{resembles}^{-1}} Compound \xrightarrow{\text{binds}} Gene \xrightarrow{\text{has link}} Gene$	1.4
	$Compound \xrightarrow{\text{upregulates}} Gene \xrightarrow{\text{has link}} Gene \xrightarrow{\text{has link}} Gene$	1.0
	$Compound \xrightarrow{\text{has mechanism}} Mechanism\ of\ Action \xrightarrow{\text{has assay target}} Gene \xrightarrow{\text{has link}} Gene$	0.8

B.2. Explanations

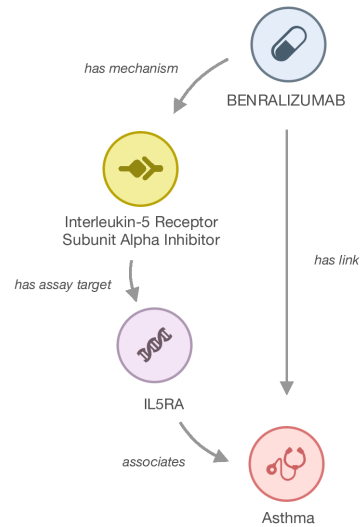


Figure 7: Explainable reasoning for recommending Benralizumab in the treatment of Asthma.

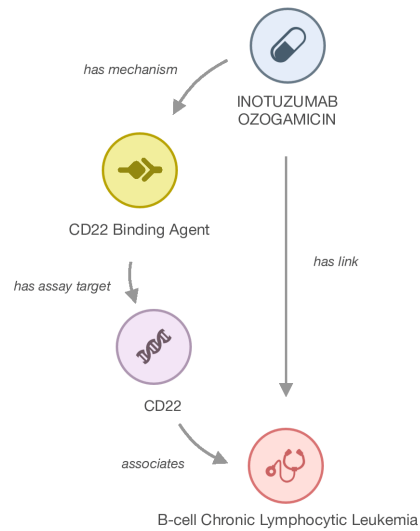


Figure 8: Explainable reasoning for recommending Inotuzumab ozogamicin in the treatment of B-cell Chronic Lymphocytic Leukemia.

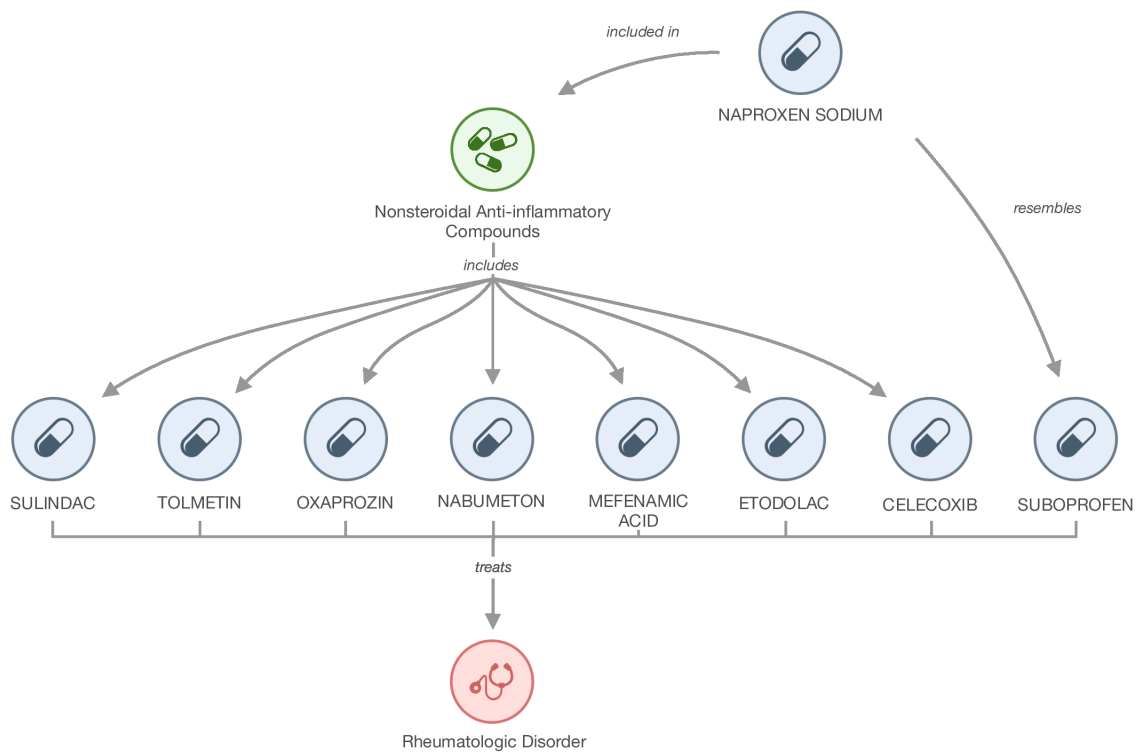


Figure 9: Explainable reasoning for recommending Naproxen Sodium in the treatment of rheumatic diseases.

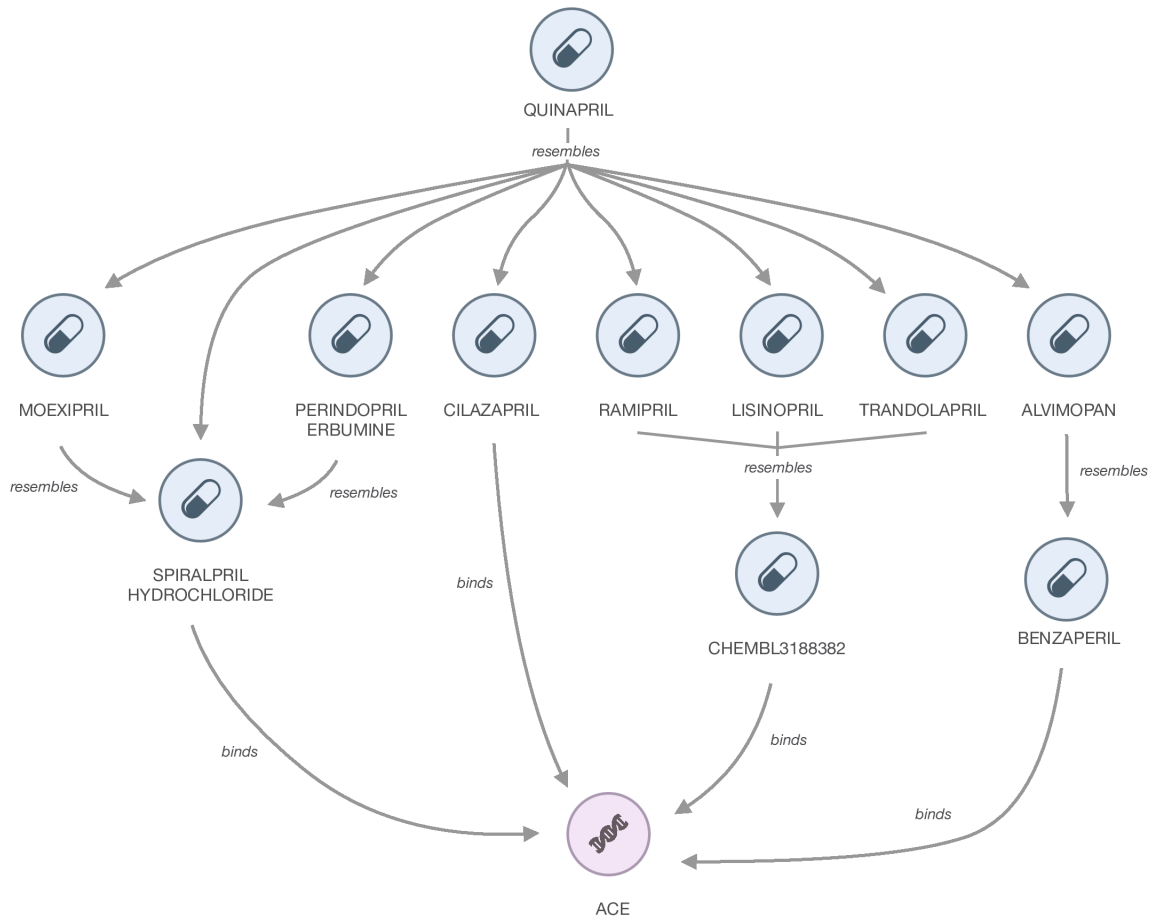


Figure 10: Explainable reasoning for recommending Quinapril as an ACE inhibitor.

Appendix C. Pre-pruned Results

Below are the results before pruning of expected target node types was applied. This effectively keeps failed walks and predictions in the results sets.

Table 11: Drug repurposing results (pre-pruning)

Dataset	Model	HITS@1	HITS@3	HITS@10	MRR
Hetionet	TransE	.193 ± .027	.364 ± .031	.608 ± .034	.312 ± .022
	DistMult	.020 ± .014	.086 ± .023	.270 ± .022	.096 ± .015
	RGCN	.053 ± .027	.200 ± .016	.454 ± .036	.217 ± .041
	AnyBURL	.116 ± .013	.288 ± .024	.572 ± .036	.258 ± .012
	MINERVA	.281 ± .027	.462 ± .055	.701 ± .055	.391 ± .034
	PoLo	.306 ± .017	.481 ± .029	.742 ± .013	.406 ± .015
BIKG Hetionet	TransE	.016 ± .003	.034 ± .005	.088 ± .001	.045 ± .004
	DistMult	.012 ± .002	.021 ± .003	.046 ± .006	.029 ± .003
	RGCN	.056 ± .005	.108 ± .008	.229 ± .011	.115 ± .004
	AnyBURL	.000 ± .000	.056 ± .005	.205 ± .014	.072 ± .002
	MINERVA	.070 ± .007	.137 ± .011	.204 ± .020	.116 ± .009
	PoLo	.089 ± .005	.162 ± .007	.239 ± .008	.142 ± .005
BIKG Hetionet+	TransE	.017 ± .002	.052 ± .004	.119 ± .011	.057 ± .002
	DistMult	.004 ± .002	.013 ± .004	.036 ± .009	.025 ± .004
	RGCN	.039 ± .008	.091 ± .014	.191 ± .012	.109 ± .060
	AnyBURL	.000 ± .000	.065 ± .006	.205 ± .008	.070 ± .009
	MINERVA	.069 ± .008	.115 ± .010	.151 ± .011	.105 ± .009
	PoLo	.068 ± .007	.117 ± .011	.157 ± .011	.105 ± .008

Table 12: Drug repurposing results (pruned)

Dataset	Model	HITS@1	HITS@3	HITS@10	MRR
Hetionet	TransE	.193 ± .027	.364 ± .031	.608 ± .034	.312 ± .022
	DistMult	.028 ± .002	.138 ± .022	.373 ± .039	.129 ± .002
	RGCN	.047 ± .028	.194 ± .018	.492 ± .043	.221 ± .040
	AnyBURL	.116 ± .013	.288 ± .024	.572 ± .036	.258 ± .012
	MINERVA	.351 ± .040	.559 ± .058	.790 ± .057	.463 ± .041
	PoLo	.378 ± .023	.575 ± .025	.845 ± .009	.479 ± .015
BIKG Hetionet	TransE	.016 ± .003	.034 ± .005	.088 ± .001	.045 ± .004
	DistMult	.004 ± .002	.013 ± .002	.036 ± .007	.024 ± .003
	RGCN	.056 ± .005	.108 ± .008	.239 ± .008	.117 ± .005
	AnyBURL	.000 ± .000	.015 ± .001	.046 ± .004	.023 ± .001
	MINERVA	.121 ± .002	.194 ± .010	.249 ± .013	.160 ± .004
	PoLo	.124 ± .005	.204 ± .010	.273 ± .016	.167 ± .008
BIKG Hetionet+	TransE	.017 ± .002	.052 ± .004	.119 ± .011	.057 ± .002
	DistMult	.004 ± .002	.014 ± .004	.039 ± .001	.026 ± .004
	RGCN	.039 ± .008	.104 ± .016	.222 ± .015	.115 ± .005
	AnyBURL	.000 ± .000	.056 ± .006	.205 ± .014	.072 ± .002
	MINERVA	.076 ± .008	.124 ± .011	.166 ± .013	.113 ± .010
	PoLo	.074 ± .006	.133 ± .010	.173 ± .012	.115 ± .007

Table 13: Drug-target interaction results (pre-pruning)

Dataset	Model	HITS@1	HITS@3	HITS@10	MRR
Hetionet	TransE	.287 ± .008	.546 ± .013	.918 ± .007	.331 ± .005
	DistMult	.037 ± .004	.120 ± .006	.355 ± .010	.111 ± .004
	RGCN	.041 ± .017	.123 ± .035	.320 ± .087	.104 ± .024
	AnyBURL	.068 ± .018	.128 ± .033	.195 ± .049	.210 ± .051
	MINERVA	<i>.159 ± .015</i>	<i>.373 ± .037</i>	<i>.756 ± .045</i>	<i>.269 ± .021</i>
BIKG Hetionet	TransE	.193 ± .010	.376 ± .012	.674 ± .012	<i>.239 ± .004</i>
	DistMult	.043 ± .007	.106 ± .015	.258 ± .016	.095 ± .007
	RGCN	.057 ± .025	.142 ± .017	.270 ± .028	.123 ± .012
	AnyBURL	.088 ± .003	.167 ± .004	.254 ± .007	.264 ± .004
	MINERVA	<i>.104 ± .011</i>	<i>.224 ± .014</i>	<i>.589 ± .013</i>	.172 ± .008
BIKG Hetionet+	TransE	.054 ± .004	.098 ± .007	.171 ± .011	.080 ± .004
	DistMult	.035 ± .006	.083 ± .011	.202 ± .028	.083 ± .001
	RGCN	<i>.058 ± .025</i>	<i>.142 ± .017</i>	.270 ± .022	<i>.123 ± .012</i>
	AnyBURL	.086 ± .002	.162 ± .003	.251 ± .007	.263 ± .003
	MINERVA	.026 ± .002	.079 ± .006	<i>.255 ± .027</i>	.085 ± .004

Table 14: Drug-target interaction results (pruned)

Dataset	Model	HITS@1	HITS@3	HITS@10	MRR
Hetionet	TransE	.287 ± .008	.546 ± .013	.918 ± .007	.331 ± .005
	DistMult	.039 ± .004	.128 ± .007	.367 ± .012	.115 ± .005
	RGCN	.060 ± .025	.177 ± .057	.376 ± .102	.126 ± .031
	AnyBURL	.169 ± .043	.323 ± .081	.493 ± .124	.210 ± .051
	MINERVA	<i>.186 ± .015</i>	<i>.420 ± .028</i>	<i>.807 ± .039</i>	<i>.296 ± .019</i>
BIKG Hetionet	TransE	.193 ± .001	.376 ± .012	<i>.674 ± .012</i>	.239 ± .004
	DistMult	.044 ± .007	.111 ± .014	.269 ± .014	.098 ± .007
	RGCN	.173 ± .016	.338 ± .013	.539 ± .021	.235 ± .008
	AnyBURL	<i>.215 ± .005</i>	<i>.408 ± .004</i>	.623 ± .009	<i>.264 ± .004</i>
	MINERVA	.235 ± .005	.516 ± .011	.983 ± .015	.305 ± .004
BIKG Hetionet+	TransE	.054 ± .004	.098 ± .007	.171 ± .011	.008 ± .004
	DistMult	.035 ± .006	.084 ± .011	.206 ± .029	.084 ± .001
	RGCN	<i>.188 ± .008</i>	.323 ± .019	.539 ± .010	.241 ± .006
	AnyBURL	.215 ± .003	.408 ± .008	<i>.622 ± .005</i>	.263 ± .003
	MINERVA	.181 ± .006	<i>.368 ± .008</i>	.628 ± .019	<i>.243 ± .004</i>